Operational issues of the ATLAS Semiconductor Tracker

**Sahal YACOOB**[*][†]

University of KwaZulu-Natal (ZA)

E-mail: Yacoob@UKZN.ac.za

Current results from the successful operation of the Semi-Conductor Tracker (SCT) Detector at the LHC and its status after three years of operation is presented. This note reports on the operation of the detector including an overview of the issues we encountered and the observation of significant increases in leakage currents from bulk damage due to non-ionising radiation. There have been a small number of significant changes effecting detector operation since the contribution to the previous conference in the series [1]. The LHC delivered 47 pb^{-1} in 2010, 5.6 fb^{-1} of proton-proton collision data in 2011 at 7 TeV and 4.06 fb^{-1} in 2012 (until September 12th) at 8 TeV, and two one-month periods of heavy ion collisions. The SCT has been fully operational throughout all data taking periods. It delivered high quality tracking data for 99.9% (2010), 99.6% (2011) and 99.3% (2012) of the recorded luminosity. The SCT running experience will be presented to extract valuable lessons for future silicon strip detector projects.

---

[*]Speaker.

[†]On behalf of the ATLAS collaboration

http://pos.sissa.it/
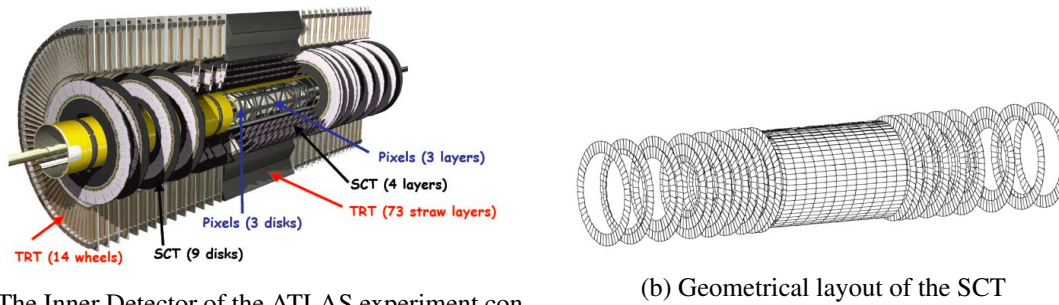
(a) The Inner Detector of the ATLAS experiment consisting of the pixel vertex detector, the silicon microstrip tracker, and the transition radiation tracker

.

(b) Geometrical layout of the SCT

.

Figure 1: The ATLAS inner detector and the geometric structure of the SCT

1. Introduction

The SCT is a silicon strip detector and one of the key precision tracking devices of the Inner Detector (ID) of the ATLAS experiment[2] at CERN's LHC. The Silicon Pixel Detector is closest to the beam-pipe and the Transition Radiation Tracker (TRT) is placed outside the SCT. The ID is operated inside a 2 T axial magnetic field and is shown in figure 1a. The SCT is constructed of 4088 silicon detector modules with 6.3 million strips representing of 61 m^2 of silicon sensors. Each module is designed, constructed and tested to operate as a stand-alone unit, mechanically, electrically, optically and thermally. The modules are mounted into two types of structures. In the central region, the barrel consists of four cylindrical layers surrounding the beam-pipe with radii ranging from 30 to 51 cm covering $|\eta| < 1.4$. On either side of the barrel are two end-cap systems, each comprised of 9 disks oriented perpendicular to the beam-pipe which extends $|\eta|$ coverage to 2.5. as shown in figure 1b with each layer traversed adding approximately 0.03 radiation lengths of material. The detector has been and installed and operated since 2007 in a nitrogen environment with close to zero humidity. The end-caps are operated at temperature of -7 °C and three of the barrel layers at -1.5 °C with the outermost barrel as warm as +4.5 °C. Temperatures are controlled by a C_3F_8 evaporative cooling system.

1.1 SCT Sensors

The SCT silicon sensors[3] are single sided p-on-n silicon sensors which are 285μm thick. Each sensor has 768 AC-coupled strips. In the barrel region all 8448 sensors (supplied b Hamamatsu) are identical rectangles of dimension 64.0x63.6mm with an 80μm strip pitch. The more complex geometry of the end-cap requires that the 6944 wedge shaped sensors have five different sizes with a strip pitch ranging from 56.9 to 90.4μm. 17.2 % of the end-cap sensors are supplied by CiS, with the remaining 82.8 % supplied by Hamamatsu.

1.2 Module Geometry

Two pairs of sensors are glued back-to-back to a thermally conductive substrate in order to form a module with the pairs on opposite sides rotated by 40 mrad allowing for the resolution in

2

(a) A module used to construct the SCT barrel layers

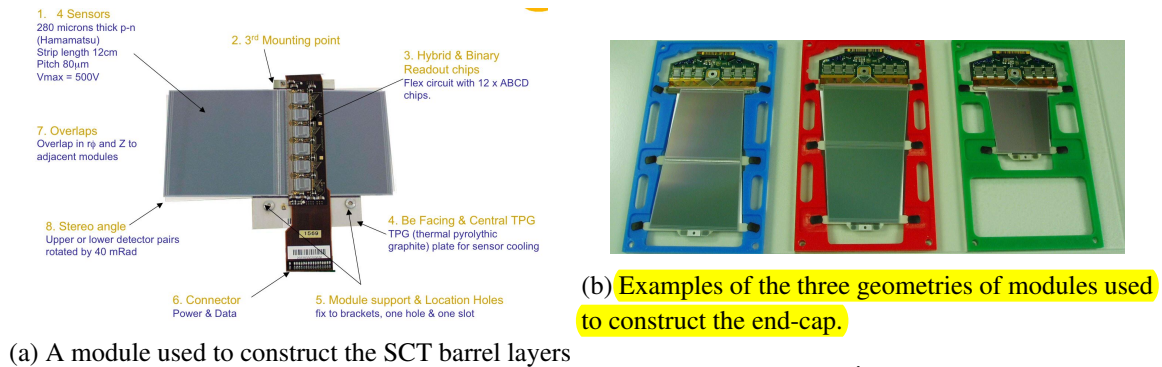(b) Examples of the three geometries of modules used to construct the end-cap.

Figure 2: The 4 types of SCT modules

the direction parallel to the strips to be determined. Adjacent micro-strips on a module are wire-bonded into 12 cm long strips in the barrel (and either 6 or 12 cm in the end-caps). The barrel modules[4] have identical geometry, while the five wedge shaped sensors of end-cap sections[5] are assembled into 3 different sizes. The Thermal Pyrolitic Graphite substrate removes the 5.6 watts of heat generated on the module. After ten years of running this s expected to rise to 10 watts. Each module may be operated at a reverse bias voltage of up to 500 V, but is nominally operated at 150 V. The voltage required for full depletion is typically 60-80 V. In order to decrease the probability of damage the bias voltage is reduced to 50 V when the LHC beams are not stable.

1.3 Module Readout

Readout is performed by six 128 channel ABCD3TA[6] ASICs per module side. The chips are manufactured using radiation hard DMILL technology. They are glued to a copper-polyimide circuit hybrid creating a bridge across the sensors. The chips are read out in binary mode with a 20 ns front end shaping time. The output from each strip is shaped, amplified, and applied to a comparator with a programmable threshold that is set to 1 fC. The comparator output is strobed at 40MHz (25 ns) in time with the LHC clock and the output is stored in a 132-deep pipeline. When the ATLAS trigger system issues a trigger, three bins of the pipe-line (centred on the bin for the bunch corresponding to the issued trigger) are read out. The ABCD will register a hit depending on the contents of these three bins. The content of each of the three time bins is 1 if there is a signal above threshold and 0 if there is no signal above threshold. For 2011 and 2012 collider data-taking the pattern in the three bins read out that would register a 'hit' was either X1X or 01X, where the 'X' means that there was no requirement on the output of this bin. For cosmic data-taking a hit in any of the three bins is sufficient.

Figure 3 shows a schematic of the SCT data acquisitions system (DAQ). The ASICs communicate with the off-detector readout electronics via optical links[7]. TX links transmit trigger and commands signals to the modules, and RX links on the modules transmit information in the other direction. Each module has 2 RX links (one per side), and up to 48 modules may be controlled by a single Read Out Driver (ROD) via TX links on the Back of Crate (BOC) card. VCSEL arrays are used to broadcast information on both TX and RX links. If a module loses a TX signal for any
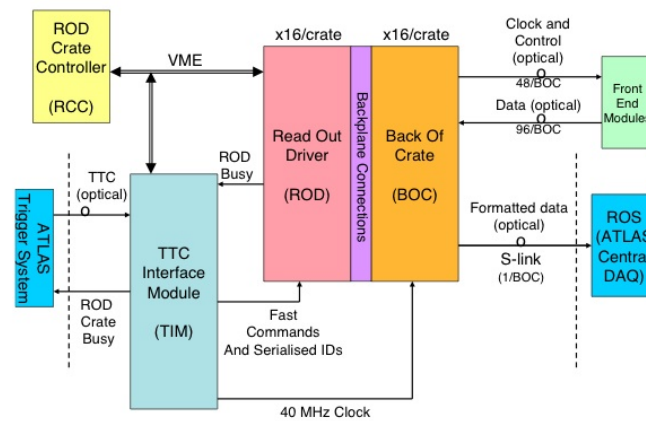
Figure 3: SCT DAQ structure.

reason it can receive signals from a neighbouring module which can be configured to send a copy of its TX data to the module which is not receiving a signal. If an RX link on a module ceases to communicate with the ROD all channels on the module can be read out via the link on the other side. In the barrel this results in the loss of one chip on the re-routed link.

2. Operations

During 2012 (until the 12$^{\text{th}}$ of September) the LHC had delivered 14.66 fb^{-1} of proton-proton collisions at 8 TeV, of which 13.73 fb^{-1} was recorded. The SCT has been fully operational delivering good tracking data for 99.3% of this period. Overall the LHC had delivered an integrated luminosity of 19.33 fb^{-1} from 2010 when this talk was presented. The SCT has been usually running at greater than 99% efficiency during this entire period. While the SCT Data Acquisition (DAQ)[8] has been reliable in order to achieve these results, part of the continued reliability has been continuous updates to the DAQ in order to improve or maintain the efficiency. A source of inefficiency are chips which become desynchronised or experience corruption of the configuration (initially loaded at the start of a physics run) due to radiation, so called single event upsets (SEUs). This effect typically effects 0.2% of the approximately 8000 data links during a period of stable running. In response to this an automatic reconfiguration of chips which exhibited this behaviour was implemented. Additionally all SCT chips now undergo an automatic reconfiguration approximately every half hour in order to protect against the effects of SEUs. There are 90 RODs in the SCT DAQ each of which processes the data for up to 48 modules, if a ROD experiences errors it will exert a BUSY signal which prevents all ATLAS sub-systems from recording data. From 2011 RODs exerting a busy were automatically removed, reconfigured, and reinserted into a run thus having a minimal impact on data taking.

A gradual and continuous increase in the leakage current for each module at both 50 and 150V has been observed. This is an expected effect of radiation damage to the SCT sensors. The 1 MeV neutron equivalent radiation fluence is measured on-detector by radiation sensitive monitors (RadMons)[9]. The measured values of the fluence and leakage current are in agreement with pre-
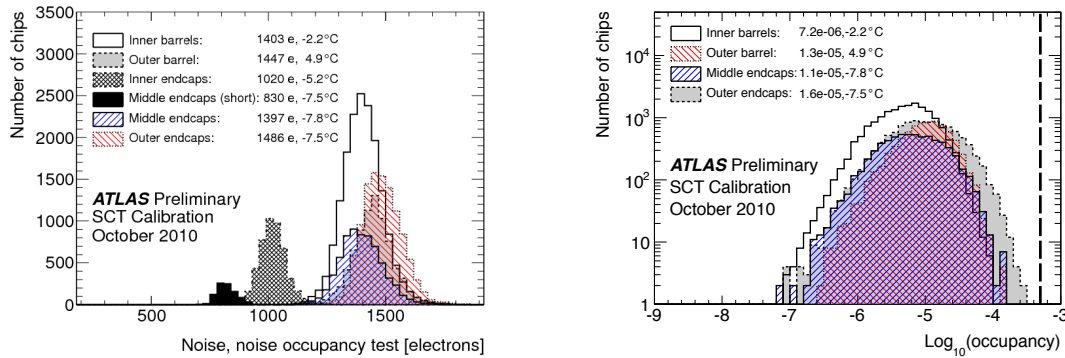
(a) Equivalent noise charge determined by the re- (b) Noise occupancy results determined by studying
sponse curve test.   hit that are isolated from particle activity.

.   .

Figure 4: Noise occupancy results[10].

dictions from a FLUKA based simulation[11] which takes into account the temperature changes
that take place during detector operation.

2.1 Noteworthy Challenges

The TX VCSEL arrays used to transmit triggers and commands to the SCT modules began
to fail several months after the onset of data-taking. The VCSEL channels died at a typical rate
of 3 to 4 deaths per day, this was a major component of SCT inefficiency until recently, although
the effects were greatly minimised by the redundancy designed into the system. The failures were
initially attributed to a lack of protection against electrostatic discharge during the manufacturing
process, and all VCSEL arrays were replaced in 2009 with units manufactured with improved pro-
tection against electrostatic discharge. Unfortunately the VCSEL channels began to fail again in
May 2010 at a rate of approximately 10 channels per week. These subsequent deaths were deter-
mined to be caused by exposure to humidity. Thus, in 2011 a new batch of TX arrays were obtained
from a different manufacturer. These TX's which were demonstrated to have a lower sensitivity to
humidity were installed to all BOCs at the end of 2011. These new VCSELs have (thus far) not
exhibited a significant failure rate, and are now operated in a lower humidity environment.
During 2012 a small number of modules (of order 100) developed anomalously high leakage cur-
rents. All affected modules had been assembled with CiS sensors. These modules continued to
be operated efficiently, but with reduced operating voltages, though care was taken to ensure the
voltages remained high enough to ensure depletion. Additionally it was necessary with some of
these modules to reduce the HV to 5V instead of 50V outside of stable beams. The cause of this
lowering of the breakdown voltage is under investigation.

3. Noise Occupancy

The ASICs on the SCT modules have charge injection circuitry which allow for a known
charge to be applied. The occupancy as a function of the discriminator threshold can be his-
togrammed (for a fixed injection charge, the discriminator threshold is varied) and fitted with a
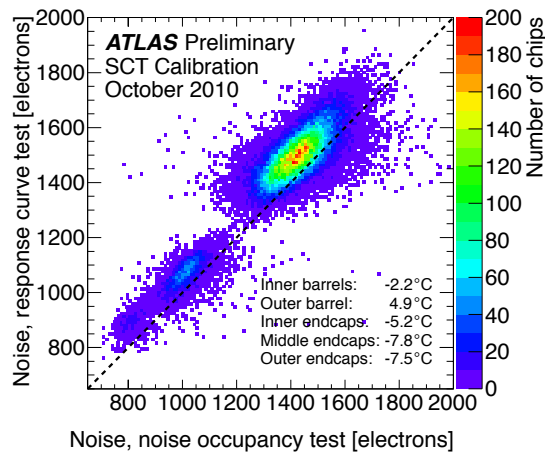
Figure 5: Comparison between the noise occupancy determined by charge injection and hits attributed to noise during detector operation[10].

.

complimentary error function. The width of the distribution is a measure of the amplified noise in mV. For a noise occupancy test this procedure is repeated for injection charges of 0.5, 0.75, 1.0, 1.25, 1.5, 2, 3, 4, 6 and 8 fC allowing for a precise determination of the gain, which allows one to determine the input noise for each channel. Values obtained are typically less than 1500 electrons, as shown in figure. 4a, which is well below the threshold of 6000. During data-taking the fraction of triggers which result in a hit when there is no particle activity in the detector can also be used to determine the noise and leads to an occupancy determination of approximately 10^{-5} (shown in figure 4b) in line with the design goal to be less than 10^{-4}. Figure 5 shows the correlation between the values obtained by each of these methods under similar running conditions in units of equivalent noise charge (ENC).

4. Alignment

Alignment is performed using an algorithm which minimises the the χ^2 between the the measured hit position and the expected position based on on track extrapolation. This is done with cosmic ray data as well as isolated high p_T tracks from collision data. Figure 6 shows the unbiased residual distributions comparing the ideal alignment from Monte-Carlo predictions with the measured values from data taken in autumn 2010. For the barrel layers (figure 6a) the measured standard deviation of the distribution was 36 μm, significantly closer to the design value of 34 μm than the value of 42 μm from measurements in May 2010. In the end-caps the standard deviation had already reached the ideal limit from Monte-Carlo predictions of 38 μm by Autumn 2010 (as shown in figure 6b).

5. Summary

The SCT has enjoyed an outstanding first two years of LHC data taking. ATLAS has had a 93.6% data taking efficiency in 2012 and greater than 99% of SCT channels have been operational

(a) SCT barrel layer residuals

(b) SCT endcap layer residuals

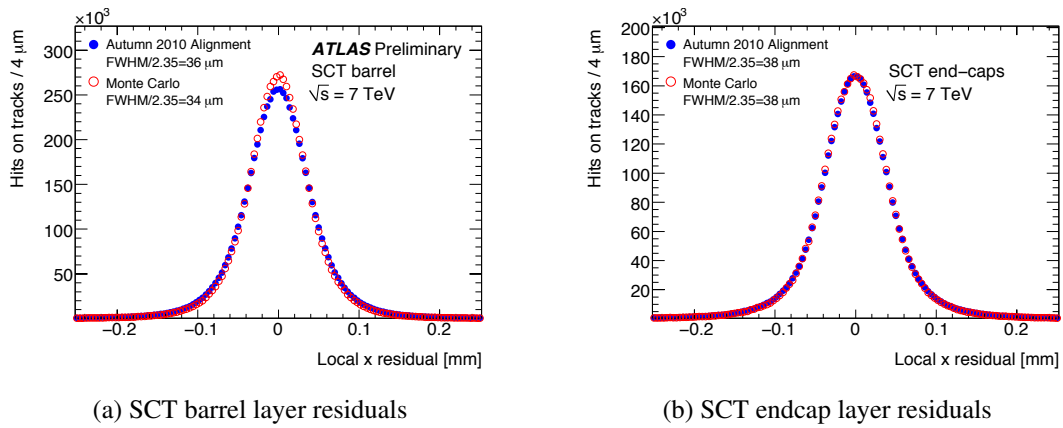.   .

Figure 6: Unbiased residual distributions for SCT barrel and endcap layers, comparing measured data with Monte Carlo simulation[12].

during this time fulfilling the design requirements. The significant effects of radiation damage are in agreement with expectations and there has only been one significant operational issue stemming from the TX VCSEL deaths. The effect of the VCSEL deaths was minimised due to the redundancy built into the readout, and the availability of replacement VCSELs.

References

[1] P. Haefner, *Operation and Performance of the ATLAS Silicon Microstrip Tracker*, in proceedings of *The 20th Anniversary International Workshop on Vertex Detectors*, 2011, `PoS (Vertex 2011) 007`

[2] The ATLAS Collaboration, G. Aad et al., *The ATLAS Experiment at the CERN Large Hadron Collider*, *JINST* **3** (2008) S08003

[3] J. Carter et al., *The silicon microstrip sensors of the ATLAS semiconductor tracker*, *Nucl. Instrum. Meth. A***578** (2007) 98-118

[4] A. Abdesselam et al., *The barrel modules of the ATLAS semiconductor tracker*, *Nucl. Instrum. Meth. A***568** (2006) 642-671

[5] A. Abdesselam et al., *The ATLAS semiconductor tracker end-cap module*, *Nucl. Instrum. Meth. A***575** (2007) 353-389

[6] F. Campabadal et al., *Design and Performance of the ABCD3TA ASIC for readout silicon strip in the ATLAS SemiConductor Tracker*, *Nucl. Inst. Meth. A***552** 2005 561

[7] T. Weidberg et al., *The optical links of the ATLAS SemiConductor Tracker*, *JINST***2** (2007) P09003

[8] A. Barr et al., *The data acquisition and calibration systm for the ATLAS Semiconductor Tracker*, *JINST* **3** (2008) P01003

[9] I. Mandic et al., *Online integrating radiation monitoring system for the ATLAS detector at the Large Hadron Collider*, *IEEE Trans. Nucl. Sci.* **54** (2007) 1143-1150

[10] The ATLAS Collaboration *Approved SCT Plots* http://twiki.cern.ch/twiki/bin/view/AtlasPublic/ApprovedPlotsSCT.

[11] A. Ferrari, P. Sala, A. Fasso and J. Ranft, *FLUKA: A multi-particle transport code*, *CERN-2005-10* 2005, *INFN/TC-05/11*, *SLAC-R-773*

[12] ATLAS Collaboration, *ATLAS note ATLAS-CONF-2011-012*

PoS(Vertex 2012)005